PHYSICAL REVIEW B **94**, 241304(R) (2016)

Structure of TiO_2 (011) revealed by photoelectron diffraction

C. Dupont,[1,*] S. Bourgeois,[1] P. Le Fèvre,[2] A. Verdini,[3] L. Floreano,[3] and B. Domenichini[1]

[1]*Laboratoire Interdisciplinaire Carnot de Bourgogne (ICB), UMR 6303 CNRS, Université Bourgogne Franche-Comté, BP 47870, 21078 Dijon Cedex, France*

[2]*Synchrotron SOLEIL, L'Orme des Merisiers, BP 48, 91192 Gif-sur-Yvette, France*

[3]*Istituto Officina dei Materiali IOM-CNR, Laboratorio TASC s.s. 14 km 163.5, 34149 Trieste, Italy*

(Received 14 October 2016; revised manuscript received 7 December 2016; published 23 December 2016)

The combination of photoelectron diffraction, density functional theory, and multiple scattering calculations is used for a quantitative analysis of the widely debated structure of TiO_2 (011). The modeling of the diffraction patterns for different surface reconstructions allows one to discriminate the key structural constraints required or, on the contrary, prohibited in the reconstruction of this termination. In particular, photodiffraction rules out previously proposed reconstructions while it evidences the key feature of the TiO_2 (011) termination: an oxygen splitting induced by missing rows.

DOI: 10.1103/PhysRevB.94.241304

I. INTRODUCTION

Since the discovery of the ability of TiO_2 to be used for photocatalytic applications such as water splitting [1], numerous studies have been dedicated to this material [2–8]. Nowadays the most stable (110) termination of the rutile form is fully characterized: Its electronic and structural properties are well known, as well as its wide range of potential applications. On the contrary, besides its potential for photocatalysis [9,10], the structure of the (011) termination is still under debate. Experimental, theoretical, and even combined studies have been performed, but a structure that reaches a general consensus has yet to be proposed. The initial investigations [11,12] proposed a "titanyl" model based on surface Ti=O groups, however, this model was rapidly refuted to give way to new hypotheses. Among them one can mainly distinguish two kinds of reconstructions: the "missing-row" models, obtained by removing atoms from the surface [13] (in the spirit of the titanyl model), and those obtained only by the rearrangement of surface atoms [14–17]. After these thorough investigations, a convergence towards the (2×1) "brookite (001)-like" (BL) reconstruction (first proposed by Torrelles *et al.* [14]) was seemingly reached, but a recent paper [18] suggested the coexistence of two phases, namely, the (4×1)-α derived from the previous model of Torrelles [14] and a new (4×1)-β phase. Beyond the reconstruction itself, this last paper has also raised the question of the nature of the second layer: Does the reconstruction occur on the native (1×1) surface or is the second layer also reconstructed? Finally, Wang *et al.* [19] have recently published a different approach for investigating the TiO_2 (011) reconstruction as they considered the influence of the partial pressure of oxygen, which allows them to consider nonstoichiometric models. Nevertheless, beyond these specific conditions, they no longer highlight only the brookite (001)-like model but they also consider the existence of missing-row and microfaceting ones.

To dispel uncertainties, we report an investigation combining techniques to resolve the reconstruction of TiO_2 (011). In this Rapid Communication, the structure of the (011) stoichiometric termination is investigated through density functional theory (DFT) and multiple scattering (MS) calculations combined with photoelectron diffraction (PED). Indeed, PED is an experimental technique particularly suited for studies of surfaces, as it probes the local order around chemically selected emitters [20,21].

II. METHOD

A. Experimental details

The experiments were performed at the ALOISA beamline [22] of the Elettra Synchrotron Light Source in Trieste, Italy. The rutile TiO_2 (011) surface was prepared, first using repeated cycles of Ar^+-ion bombardments (1 keV) and annealing at 973 K in order to create conductivity in material bulk via oxygen deficiencies, and then removing any charge effect under the photoemission process. Contrary to previous studies [11,13,14,17,18] which performed the whole preparation process under UHV, our last annealing was carried out under O_2 (pressure of about 10^{-4} Pa) at 723 K for 15 min, in order to reoxidize the topmost layers. This preparation ensures a stoichiometric surface and thus allows an accurate comparison with calculations. The surface is then controlled by reflection high energy electron diffraction (RHEED) in order to reveal the main surface orientations and to check the degree of ordering from the spot width. In fact, the good quality of the surface is also evidenced by the high modulation of PED data (around 50%, see below). In addition, we paid attention to the surface stoichiometry as monitored by the Ti^{3+} $3d$ states just below the Fermi level, which exhibit a strong resonance behavior when the photon energy goes through the Ti $L_{2,3}$ edges [23]. After O_2 treatment, no Ti^{3+} $3d$ states were detectable at resonance. For PED experiments, the x-ray beam was impinging on the sample at grazing incidence (4°) with light polarization normal to the surface. Photoemission intensities were recorded as a function of polar (θ) and azimuthal (ϕ) angles. Photoelectron diffraction spectra were measured at room temperature for photoelectrons from the Ti $2p$ core level with a kinetic energy of 464 eV. For the analysis we evaluate the anisotropy function $\chi(\theta,\phi) = [I(\theta,\phi) - I_0(\theta)]/I_0(\theta)$, where $I_0(\theta)$ is the

*celine.dupont@u-bourgogne.fr

ϕ average of $I(\theta,\phi)$ and represents the smoothly varying isotropic function, as originated by both instrumental details (illuminated area) and physical properties (atomic angular cross section, escape depth, surface roughness) [24]. We call the PED pattern the stereographic $\chi(\theta,\phi)$ plot. The difference between two patterns χ_A and χ_B can be quantified from the R factor, $R_f = \sum(\chi_A - \chi_B)^2 / \sum(\chi_A^2 + \chi_B^2)$, where the sum is performed over the entire experimental angular range. In this case, $\theta = 0^\circ \rightarrow 69^\circ$, where 0° is along the surface normal and $\phi = 0^\circ \rightarrow 90^\circ$, between the two symmetry directions. $R_f = 0$ and $R_f = 1$ correspond to identical and uncorrelated data sets, respectively.

B. Computational details

In order to determine the optimal reconstruction, periodic density functional theory calculations have been performed using the VASP package [25,26]. All reconstructions have been modeled with symmetric slabs of 11 layers of TiO_2 [corresponding to a slab thickness of 27.2 Å for the native TiO_2 (011) slab] reconstructed on both sides to avoid any spurious dipolar moment. The large thickness of 11 layers has been chosen to allow a high convergence of the surface reconstruction. Total energy calculations have been performed following the generalized gradient approximation (GGA)+U with the Perdew-Burke-Ernzerhof (PBE) functional [27], and a value of 4.2 eV for U in Dudarev's approach [28]. The projector augmented-wave (PAW) method has been used, with 12 valence electrons for Ti (namely, $3s^2$, $3p^6$, $4s^2$, and $3d^2$) and six for O (namely, $2s^2$ and $2p^4$) and a converged plane-wave cutoff of 500 eV has been applied. The Brillouin zone integration has been performed with a $(3\times3\times1)$ Monkhorst-Pack k-point mesh. The geometry optimization has been completed when forces becomes smaller than 0.01 eV Å^{-1}. With these settings, the numerical error on the total energy is lower than 0.01 eV. Experimentally, a kinetic energy of the emitted electrons of 464 eV has been used corresponding to an inelastic mean free path of 12 Å [29], i.e., an analysis thickness spread over 15 atomic layers, namely, five TiO_2 layers. Once stable structures were obtained, the corresponding PED patterns were modeled by performing multiple scattering calculations using the EDAC code [30], within the cluster approach. To allow accurate comparisons, fixed clusters of 375 atoms have been used in all cases.

III. RESULTS

In order to evidence the main characteristics of the (011) termination, numerous reconstructions (18), including all structures previously proposed in the literature, have been modeled. In particular, the widely reported BL [14,15] has been considered, as well as the first proposed titanyl model [11]. The microfacet (MF) model proposed by Kubo *et al.* [13] has been adapted in order to make it stoichiometric and thus has also been investigated within the two periodicities, namely, (2×1) and a (4×1). In particular, to preserve the stoichiometry, Ti_2O_4 rows have been removed, instead of Ti_2O_2. Finally, in agreement with the paper of Pang *et al.* [18], the (4×1)-α, the (4×1)-β, and multilayer models have been considered. For this last case, we mainly optimized combinations of the MF and the BL model. Different arrangements have been considered depending on the first layer and second layer reconstruction (namely, layer 1 = MF/layer 2 = MF or layer 1 = MF/layer 2 = BL or layer 1 = BL/layer 2 = MF) and through the combination of different periodicities. Their relative stability has been considered through their surface energy (see Table I) and their corresponding photoelectron diffraction patterns have been calculated.

TABLE I. Surface energy in meV/A^2 and reliability factor for different models for the rutile (011) termination. MF stands for microfacet, while BL stands for brookitelike.

Model	Surface energy (meV/A^2)	R_f
BL model [Fig. 2(c)] [14,15,17]	92	0.78
Native (011) [Fig. 1(b)]	99	0.66
Multilayer: MF/BL	104	0.79
Titanyl model [11,12]	109	0.81
MF-4×1 [Fig. 2(b)] (adapted from Ref. [13])	110	0.57
Multilayer: MF/MF	110	0.63
MF-2×1 (adapted from Ref. [13])	113	0.67
(4×1)-α model [18]	119	0.74
Multilayer: BL/MF	119	0.86
(4×1)-β model [18]	125	0.77

First of all, the experimental PED data set, as well as the calculated one of the nonreconstructed (011) termination, are reported in Fig. 1. Since the angular position of the focusing peaks in PED patterns is well known to provide short-range information on the structure of the topmost layers [20,21], a few qualitative conclusions can be drawn from a visual comparison of the patterns. Especially, we notice a remarkable agreement between the main diffraction features and the calculated ones for a nonreconstructed termination. Nevertheless, some discrepancies become evident upon quantitative analysis. Among them, one can mention the case of features A and B. Experimentally, they present an identical intensity, while on the calculated PED spectrum of native (011), the B feature is of very low intensity compared to A. This is also the case for the C feature, which presents a much lower intensity in the calculated patterns. On the contrary, the central G feature is more pronounced on the calculated pattern rather than on the experimental one. Finally, one can observe the additional F point as well as a spurious mark below the I feature, on the calculated anisotropy pattern of the nonreconstructed surface.

From our calculations the titanyl model [11,12] can be immediately excluded. Its PED pattern [see Fig. 2(c)] leads to a large R_f of 0.81. This is mainly due to the large central spot, which encompasses both A and B diffraction points and almost extends to the D feature. Other imprecisions can be mentioned, such as the E feature presenting a too large value of ϕ and the large intensity of the G feature. This very poor agreement confirms previous studies [13,14] which have already dismissed this model. A second unsuitable model is the (4×1)-β recently proposed by Pang *et al.* [18]. The structure as reported in Ref. [18] is nonstoichiometric, hence several attempts have been made to reproduce similar reconstruction patterns in a stoichiometric configuration. The most stable case leads to a calculated surface energy of 125 meV A^{-2}

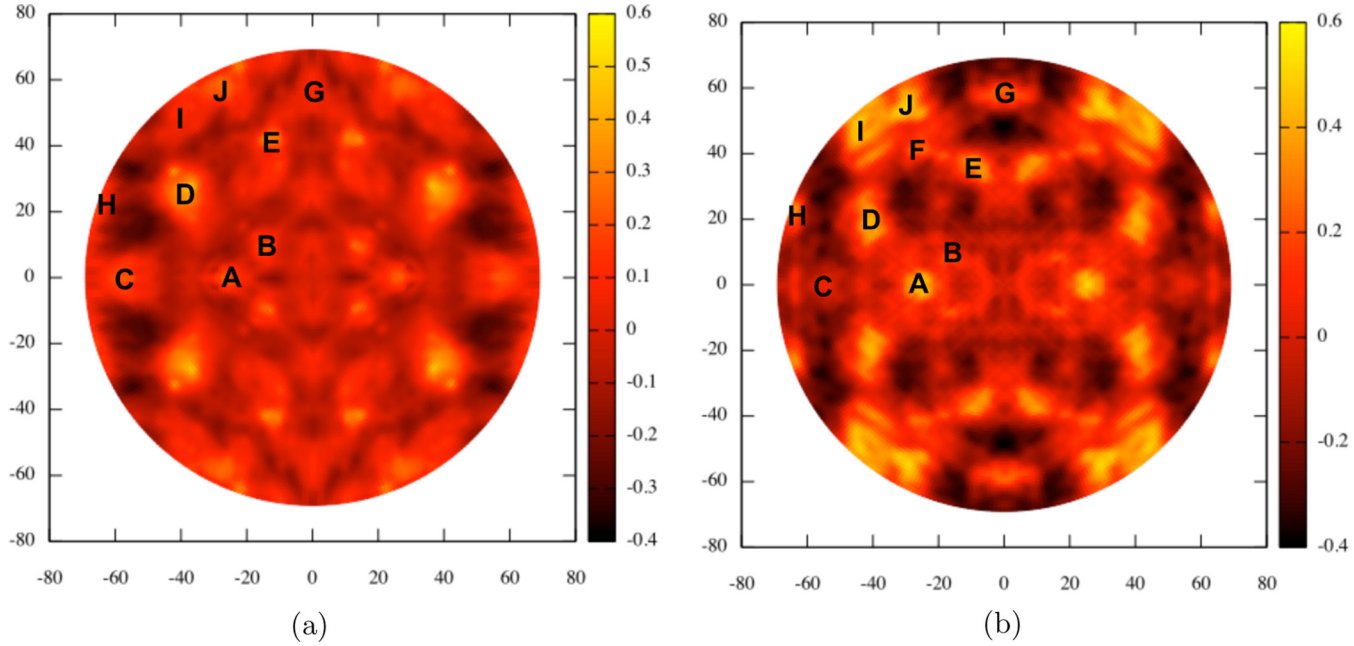

FIG. 1. (a) Experimental photoelectron diffraction (PED) pattern $\chi(\theta,\phi)$, from the Ti $2p$ core level. The main diffraction points are denoted from A to G. (b) Calculated photoelectron diffraction pattern for the nonreconstructed TiO_2(011) termination (the corresponding structure is reported in Fig. S1 of the Supplemental Material [31]). The projection is linear in θ with the surface normal ($\theta = 0$) in the center. $\phi = 0$ ($\phi = 90$) is found a 3 o'clock (12 o'clock) and corresponds to the $[\bar{1}00]$ ($[0\bar{1}\bar{1}]$) direction.

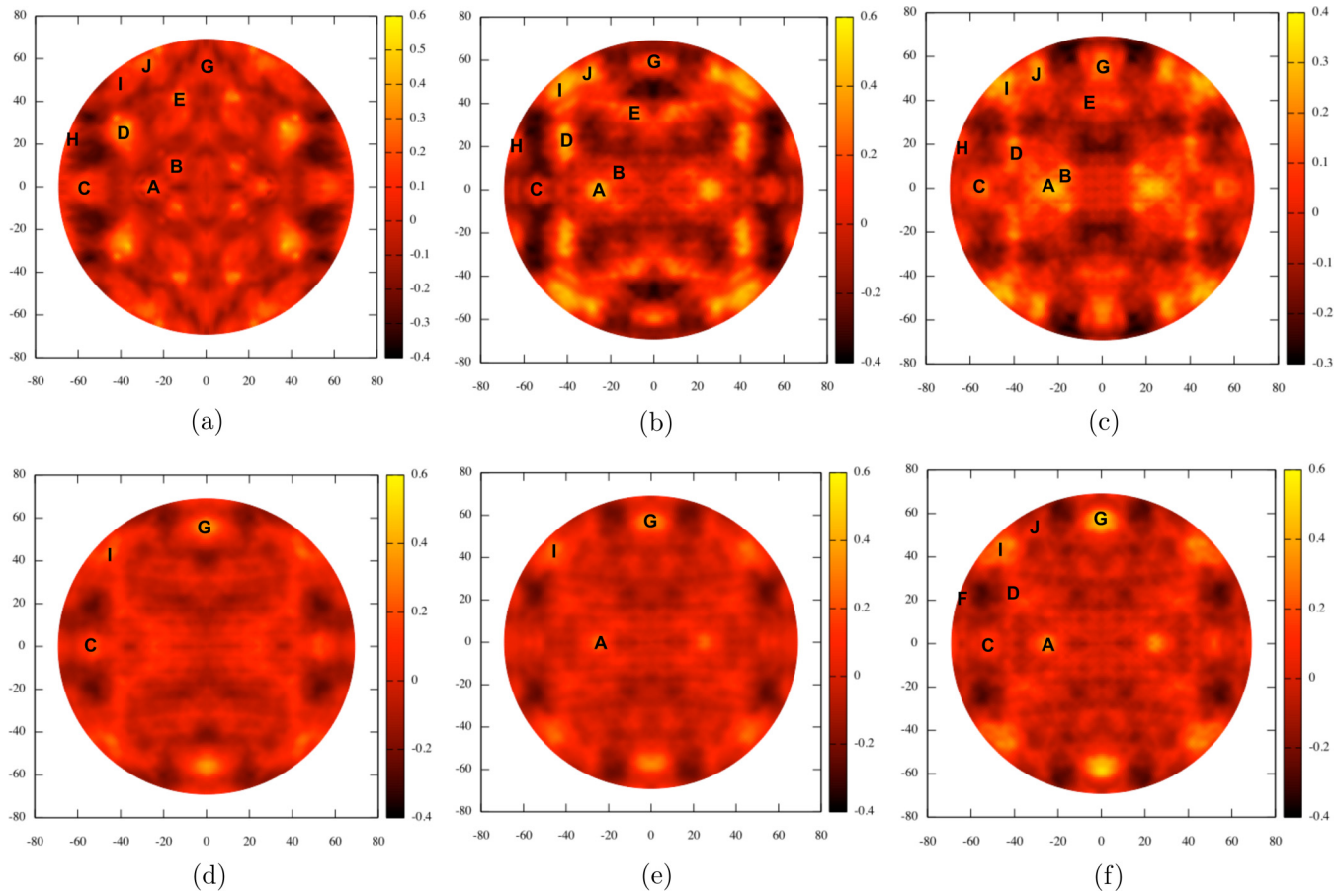

FIG. 2. (a) Experimental photoelectron diffraction (PED) patterns $\chi(\theta,\phi)$, from the Ti $2p$ core level. Calculated photoelectron diffraction patterns for (b) the stoichiometric microfacet (4×1) reconstruction, (c) the titanyl model, (d) the (4×1)-α from Ref. [18], (e) (4×1)-β from Ref. [18], and for (f) the brookite (001)-like model. The main diffraction points are denoted from A to G. Corresponding structures for (c), (d), (e), and (f) are reported un Figs. S2–S5 of the Supplemental Material, respectively.

(see Table I), namely, 25% less stable than the native termination. This large surface energy is heightened by a high R_f of 0.77 due to a large G spot and features B, D, E, and J being almost non existent [see Fig. 2(e)]. The same conclusions can be drawn for the (4×1)-α still proposed by Pang *et al.* [18]. In fact, this model is just slightly more stable than the (4×1)-β, with a surface energy of 119 meV A^{-2}, but it also presents a high R_f of 0.74, with a similar fla t appearance of the PED pattern [see Fig. 2(d)].

Based on these first conclusions, we focus on the BL model proposed by the group of Thornton [14] and the one of Diebold [15] and on the stoichiometric microfacet one developed here by adapting the model of Nozoye *et al.* [13]. Given the fairly low differences in surface energies between these different reconstructions, all included in a 10% range around the surface energy of the native termination (see Table I), the only consideration of the stability is not sufficient to discriminate a model among the others. Hence we will mainly discuss PED patterns and the corresponding reliability factors.

According to Table I, all reconstructions, except those derived from the MF model, present a reliability factor higher than the one of the native termination. In particular, this is the case of the widely accepted BL model, with $R_f = 0.78$. Beyond this low quantitative agreement, qualitatively the PED spectra of the BL model presents two major defects: The B feature is missing, while the G feature is far too intense [see Fig. 2(f)]. This large intensity is due to a combination of two phenomena. In fact, G is already present in the native termination, where it can be attributed to the scattering between two titanium atoms in two standard rutile layers. Apart from the rearrangement of the surface layer, the BL model is constituted of standard rutile layers which contribute to G. Besides this titanium-titanium diffraction, the specific rearrangement of the BL model leads to a Ti-O diffraction from a titanium atom of the relaxed layer. This surface diffraction certainly yields the main contribution to G.

Following this analysis based on the R_f, the stoichiometric MF model with (4×1) periodicity appears to be the best model for TiO_2 (011) termination. This is confirmed by the qualitative appearance of the PED spectra reported in Fig. 2(b). Hence the main weaknesses of the nonreconstructed termination and of the BL model simulations are improved: The B feature appears with a more pronounced intensity, as well as the C feature, whereas the intensity of G is reduced. All these changes can be explained owing to the specific multifacet reconstruction reported in Fig. 3 while its main geometric characteristics are detailed in Table II. Hence, the key feature which explains the low R_f is the presence of point B. This contribution is specific to this reconstruction and can be seen as a split of feature A. In fact, A is due to Ti-O scattering from titanium atoms of the second layer on oxygen atoms of the sublayer, such as Ti_{11}-O_9, Ti_{12}-O_{10}, Ti_{13}-O_{11}, and Ti_{14}-O_{12} (see Fig. 3). B also comes from the same kind of Ti-O diffraction, but related to atoms at the edge of the reconstruction, namely, Ti_7-O_7 and Ti_{10}-O_8. In fact, while in nonreconstructed areas the oxygen atoms of the sublayer stand right above the titanium atoms of the second layer within the same $(01\bar{1})$ plane (see, for example, O_9 over Ti_{11} in Fig. 3), at the edge of the reconstruction a slight transverse shift of the oxygen atom can be observed. This is

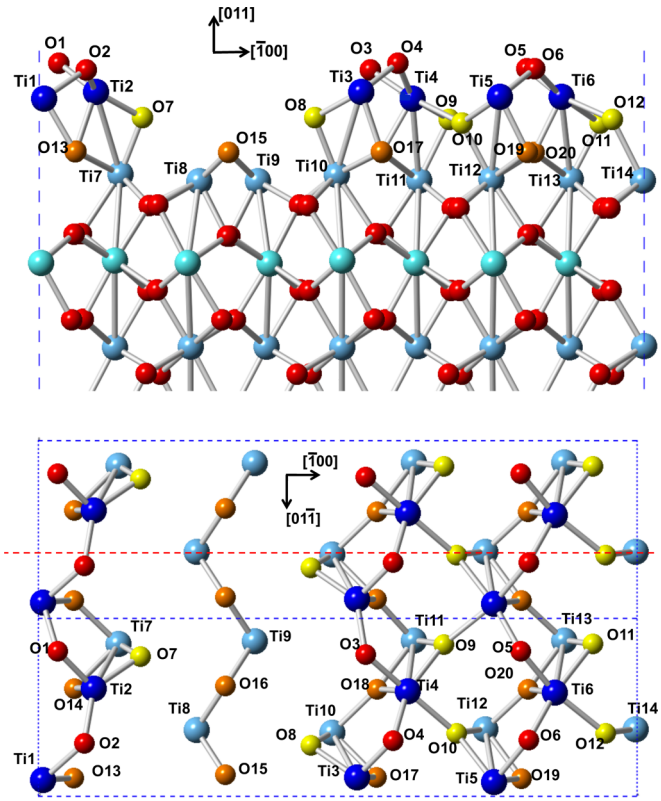

FIG. 3. Side view (top) and top view (bottom) of the stoichiometric microfacet reconstruction. Titanium atoms are reported in different shades of blue, while oxygen atoms are in red, yellow, and orange, depending on their layer. The main atoms are numbered. Blue dashed lines represent the cell used for DFT calculations, defined with the following parameters: $a = 18.372$ Å, $b = 5.463$ Å, and $c = 45.000$ Å.

TABLE II. Values for main distances (in Å) and angles (in degrees). The numbering of atoms refers to Fig. 3.

Bond	d (Å)	Bond	d (Å)	Angle	(deg)
Ti_1-O_1	1.90	Ti_8-O_{15}	1.87	Ti_1-O_1-Ti_2	111
Ti_1-O_2	1.91	Ti_8-O_{16}	1.84	Ti_1-O_2-Ti_2	119
Ti_2-O_1	1.82	Ti_9-O_{15}	1.84	Ti_3-O_3-Ti_4	119
Ti_2-O_2	1.84	Ti_9-O_{15}	1.84	Ti_3-O_4-Ti_4	111
Ti_3-O_3	1.84	Ti_9-O_{16}	1.87	Ti_5-O_5-Ti_6	124
Ti_3-O_4	1.82	Ti_{10}-O_8	1.90	Ti_5-O_6-Ti_6	124
Ti_4-O_3	1.91	Ti_{10}-O_{17}	2.05	Ti_7-O_{13}-Ti_{14}	134
Ti_4-O_4	1.90	Ti_{10}-O_{18}	2.03	Ti_7-O_{14}-Ti_{14}	132
Ti_5-O_5	1.87	Ti_{11}-O_9	2.08	Ti_8-O_{15}-Ti_9	123
Ti_5-O_6	1.87	Ti_{11}-O_{17}	1.92	Ti_8-O_{16}-Ti_9	123
Ti_6-O_5	1.87	Ti_{11}-O_{18}	2.07	Ti_{10}-O_{17}-Ti_{11}	132
Ti_6-O_6	1.87	Ti_{12}-O_{10}	1.93	Ti_{10}-O_{18}-Ti_{11}	135
Ti_7-O_7	1.90	Ti_{12}-O_{19}	2.04	Ti_{12}-O_{19}-Ti_{13}	131
Ti_7-O_{13}	2.03	Ti_{12}-O_{20}	1.96	Ti_{12}-O_{20}-Ti_{13}	131
Ti_7-O_{14}	2.06	Ti_{13}-O_{11}	1.93	Ti_2-Ti_7-O_7	38
Ti_{14}-O_{12}	2.08	Ti_{13}-O_{19}	1.96	Ti_6-Ti_{13}-O_{11}	43
Ti_{14}-O_{13}	2.07	Ti_{13}-O_{20}	2.04		
Ti_{14}-O_{14}	1.92	Ti_{13}-O_{20}	2.04		

clearly evidenced by the red dotted line on the bottom part of Fig. 3. While O_{10} and O_{12} (respectively O_9 and O_{11}) are perfectly lined up with Ti_8, Ti_{10}, Ti_{12}, and Ti_{14} (respectively Ti_7, Ti_9, Ti_{11}, and Ti_{13}), O_8 (respectively O_7) is moved away from Ti_{10} (respectively Ti_7). This is also traduced by the decrease of the $\widehat{\text{Ti-Ti-O}}$ angle, from 43° for $\widehat{Ti_6\text{-}Ti_{13}\text{-}O_{11}}$ to 38° for $\widehat{Ti_2\text{-}Ti_7\text{-}O_7}$. A second benefit of this reconstruction is to increase the intensity of feature C. Likewise A and B, it comes from a Ti-O diffraction from the second titanium layer to oxygen sublayer but now with a gap between titanium and oxygen. Among others, C is due to the following scattering paths: Ti_7-O_{11}, Ti_8-O_8, Ti_9-O_9, Ti_{11}-O_{11}, Ti_{13}-O_7, ... Hence, the presence of the missing row induces an increase in the intensity of scattering from the oxygen atoms protruding over the troughs, such as O_7 and O_8. Finally, we evidenced that the MF (4×1) model allows one to decrease the intensity of the G feature. As mentioned previously in the case of the BL model, G is due to a Ti-Ti diffraction between two standard rutile layers, such as, for example, Ti_{11}-Ti_4. In the case of our MF model, the missing row removes two diffraction channels, those due to Ti_8 and Ti_9, inducing a decrease in intensity for the G feature.

In agreement with the study of Kubo *et al.* [13], we have also considered the MF model with a (2×1) periodicity. As for the (4×1) MF model fully described above, we removed TiO_2 rows, but one out of two instead of one out of four. According to Table I, this leads to a increase of R_f from 0.57 to 0.67, a value similar to those of the non-native TiO_2 (011) termination. This is directly related to the B feature. In fact, with this high density of missing rows, the transverse shift of the edge oxygen atoms is no longer observed and all sublayer oxygen atoms remain within the $(01\bar{1})$ plane of the corresponding titanium atom underneath.

Finally, the case of the multilayer model, namely, when the reconstruction occurs over an already reconstructed platform, is discussed, according to the recent paper of Pang *et al.* [18]. As mentioned above, different combinations of our MF model and the BL one have been considered. From the results reported in Table I, one can conclude that the presence of a second layer already reconstructed does not lead to drastic changes, either for the surface energy or for the reliability factor. Multilayers can be seen as an average of the models from which they derive. Hence the presence of these multilayer models does not introduce any new geometrical characteristic and thus no new diffraction patterns. If they are experimentally observed, this might be explained as related to a residual roughness after surface preparation, rather than to a real physical stability. To evaluate the presence or absence of these multilayer models in our specific case, we perform a quantitative analysis through the reliability factor (R_f). More precisely, we combine several reconstruction models and determine which weight of each model leads to the lowest R_f. This careful analysis does not lead to any significant improvement, as only a small decrease of R_f from 0.57 for the (4×1) MF to 0.56 is observed when we introduce a contribution of 14% of the multilayer MF/MF model.

IV. CONCLUSION

In summary, this structural investigation with a chemically selective technique such as PED brings a deeper understanding of rutile (011) surface reconstruction. In particular, the widely discussed brookite (001)-like model is rejected given its divergence, both quantitatively and qualitatively, with the experimental PED spectra. On the contrary, we demonstrate that our stoichiometric adaptation of the previously proposed microfacet model is a reconstruction able to explain the specific A/B splitting feature observed on the experimental PED spectra. The unique shift of oxygen atoms at the edge of the missing row is responsible for the presence of the B feature. Owing to photoelectron diffraction, it is now proved that the TiO_2 (011) termination is composed of missing rows, explained by a microfaceting model.

ACKNOWLEDGMENT

Calculations were performed using HPC resources from DSI-CCUB (Université de Bourgogne) and IDRIS (CNRS-Paris) resources.

[1] A. Fujishima and K. Honda, Nature (London) **238**, 37 (1972).
[2] D. A. Tryk, A. Fujishima, and K. Honda, Electrochim. Acta **45**, 2363 (2000).
[3] J. H. Park, S. Kim, and A. J. Bard, Nano Lett. **6**, 24 (2006).
[4] M. Matsuoka, M. Kitano, M. Takeuchi, K. Tsujimaru, M. Anpo, and J. M. Thomas, Catal. Today **122**, 51 (2007).
[5] A. Fujishima, X. Zhang, and D. A. Tryk, Surf. Sci. Rep. **63**, 515 (2008).
[6] J. Gong, Y. Lai, and C. Lin, Electrochim. Acta **55**, 4776 (2010).
[7] X. Chen, S. Shen, L. Guo, and S. S. Mao, Chem. Rev. **110**, 6503 (2010).
[8] M. A. Henderson, Surf. Sci. Rep. **66**, 185 (2011).
[9] T. Ohno, K. Sarukawa, and M. Matsumura, New J. Chem. **26**, 1167 (2002).
[10] J. Tao, T. Luttrell, and M. Batzill, Nat. Chem. **3**, 296 (2011).
[11] T. J. Beck, A. Klust, M. Batzill, U. Diebold, C. Di Valentin, and A. Selloni, Phys. Rev. Lett. **93**, 036104 (2004).
[12] O. Dulub, C. D. Valentin, A. Selloni, and U. Diebold, Surf. Sci. **600**, 4407 (2006).
[13] T. Kubo, H. Orita, and H. Nozoye, J. Am. Chem. Soc. **129**, 10474 (2007).
[14] X. Torrelles, G. Cabailh, R. Lindsay, O. Bikondoa, J. Roy, J. Zegenhagen, G. Teobaldi, W. A. Hofer, and G. Thornton, Phys. Rev. Lett. **101**, 185501 (2008).
[15] X. Gong, N. Khorshidi, A. Stierle, V. Vonk, C. Ellinger, H. Dosh, H. Cheng, A. Selloni, Y. He, O. Dulub, and U. Diebold, Surf. Sci. **603**, 138 (2009).
[16] S. E. Chamberlin, C. J. Hirschmugl, H. C. Poon, and D. K. Saldin, Surf. Sci. **603**, 3367 (2009).
[17] T. Woolcot, G. Teobaldi, C. L. Pang, N. S. Beglitis, A. J. Fisher, W. A. Hofer, and G. Thornton, Phys. Rev. Lett. **109**, 156105 (2012).
[18] C. L. Pang, A. Yurtsever, J. Onoda, Y. Sugimoto, and G. Thornton, J. Phys. Chem. C **118**, 23168 (2014).

[19] Q. Wang, A. Oganov, O. Feya, Q. Zhu, and D. Ma, Phys. Chem. Chem. Phys. **18**, 19549 (2016).
[20] C. Westphal, Surf. Sci. Rep. **50**, 1 (2003).
[21] C. Fadley, in *Synchrotron Radiation Research: Advances in Surface and Interface Science*, edited by R. Z. Bachrach (Plenum, New York, 1992), Vol. 1, p. 421.
[22] L. Floreano, G. Naletto, D. Cvetko, R. Gotter, N. Malvezzi, L. Marassi, A. Morgante, A. Santaniello, A. Verdini, F. Tommasini, and G. Tondello, Rev. Sci. Instrum. **70**, 3855 (1999).
[23] P. Le Fèvre, J. Danger, H. Magnan, D. Chandesris, J. Jupille, S. Bourgeois, M.-A. Arrio, R. Gotter, A. Verdini, and A. Morgante, Phys. Rev. B **69**, 155421 (2004).
[24] F. Bruno, L. Floreano, A. Verdini, D. Cvetko, R. Gotter, A. Morgante, M. Canepa, and S. Terreni, J. Electron. Spectrosc. Relat. Phenom. **127**, 85 (2002).
[25] G. Kresse and J. Hafner, Phys. Rev. B **47**, 558 (1993).
[26] G. Kresse and J. Furthmüller, Phys. Rev. B **54**, 11169 (1996).
[27] J. P. Perdew, K. Burke, and M. Ernzerhof, Phys. Rev. Lett. **77**, 3865 (1996).
[28] S. L. Dudarev, G. A. Botton, S. Y. Savrasov, C. J. Humphreys, and A. P. Sutton, Phys. Rev. B **57**, 1505 (1998).
[29] S. Tanuma, C. J. Powell, and D. R. Penn, Surf. Interf. Anal. **21**, 165 (1993).
[30] F. J. Garcia de Abajo, M. A. Van Hove, and C. S. Fadley, Phys. Rev. B **63**, 075404 (2001).
[31] See Supplemental Material at http://link.aps.org/supplemental/10.1103/PhysRevB.94.241304 for structures of the titanyl model, the (4×1)-α, the (4×1)-β and the "brookite (001)-like" model.